Impairment of IGF-I expression and anabolic signaling following ischemia/reperfusion in skeletal muscle of old mice

David W. Hammers[1], **Ronald W. Matheny Jr.**[2], **Christian Sell**[3], **Martin L. Adamo**[2], **Thomas J. Walters**[4], **J. Scot Estep**[5], and **Roger P. Farrar**[1]

[1] Department of Kinesiology, The University of Texas, 1 University Station D3700, Austin, TX 78712

[2] Department of Biochemistry and the Sam and Ann Barshop Institute for Longevity and Aging Studies, The University of Texas Health-Science Center in San Antonio, 7703 Floyd Curl Dr, San Antonio, TX 78229

[3] Department of Pathology, Drexel University College of Medicine, 245 N 15th St, Philadelphia, PA 19102

[4] Regenerative Medicine, US Army Institute of Surgical Research, 3400 Rawley E. Chambers Ave., Fort Sam Houston, TX 78234-6315

[5] Comparative Pathology, US Army Institute of Surgical Research, 3400 Rawley E. Chambers Ave., Fort Sam Houston, TX 78234-6315

Abstract

With the advancement of age, skeletal muscle undergoes a progressive decline in mass, function, and regenerative capacity. Previously, our laboratory has reported an age-reduction in recovery and local induction of IGF-I gene expression with age following tourniquet (TK)-induced skeletal muscle ischemia/reperfusion (I/R). In this study, young (6 mo) and old (24–28 mo) mice were subjected to 2 hours of TK-induced ischemia of the hindlimb followed by 1, 3, 5, or 7 days of reperfusion. Real time-PCR analysis revealed clear age-related reductions and temporal alterations in the expression of IGF-I and individual IGF-I Ea and Eb splice variants. ELISA verified a reduction of IGF-I peptide with age following 7 days recovery from TK. Western blotting showed that the phosphorylation of Akt, mTOR, and FoxO3, all indicators of anabolic activity, were reduced in the muscles of old mice. These data indicate an age-related impairment of IGF-I expression and intracellular signaling does exist following injury, and potentially has a role in the impaired recovery of skeletal muscle with age.

Keywords

Tourniquet; sarcopenia; muscle regeneration; mTOR; FoxO

NIH-PA Author Manuscript

INTRODUCTION

Sarcopenia is the progressive decline in skeletal muscle mass and function with advanced aging (See Adamo and Farrar, 2006; Conboy and Rando, 2005 for review). The skeletal muscle of aged individuals also demonstrates more susceptibility to injury (Brooks and Faulkner, 1996; Zerba et al., 1990) and impaired regeneration following injury (Brooks and Faulkner, 1990; Hammers et al., 2008; Sadeh, 1988), suggesting that these characteristics are included in the sarcopenic phenotype. Investigations of muscle regeneration in heterochronic muscle transplantation (Carlson and Faulkner, 1989) and parabiosis (Conboy et al., 2005) models demonstrate that muscles of aged animals regenerate similarly as those of young when exposed to a young systemic environment. This indicates that diffusible, extrinsic factors have a substantial influence on intrinsic cellular processes in the age-related decline in muscle regenerative capacity, and suggests autocrine/paracrine growth factor(s), such as IGF-I, play a role in this phenomenon.

Surgical use of pneumatic tourniquets (TK) on the extremities occurs over 20,000 times a day worldwide (McEwen and Inkpen, 2004). Their prolonged use results in a severe ischemia reperfusion (I/R) injury of the affected skeletal muscle (Blaisdell, 2002), defining a very clinically-relevant problem. Considering the large proportion of orthopedic surgeries performed on elderly individuals, the extent of damage and subsequent recovery of aged skeletal muscle from TK-induced I/R is a topic of importance. Our laboratory has shown that skeletal muscles of aged rats have greater functional deficits than young following 7 and 14 days of recovery from TK-induced I/R injury, and an age-associated defect in the local induction of IGF-I is a potential mechanism contributing to this phenomenon (Hammers et al., 2008).

Local induction of IGF-I in skeletal muscle occurs in various models of muscle injury (Edwall et al., 1989; Hayashi et al., 2004; Hill and Goldspink, 2003; Hill et al., 2003; Jennische and Hansson, 1987; Jennische et al., 1987). The role IGF-I plays in injured muscle includes cell survival, satellite cell proliferation, and satellite cell differentiation (See Adamo and Farrar, 2006; Adams, 2002; Charge and Rudnicki, 2004 for review). A splice variant of IGF-I mRNA encoding pro-IGF-I Eb is reported to be increased over control levels during the period corresponding to the satellite cell proliferative phase after injury (Hill and Goldspink, 2003; Hill et al., 2003). Conversely, these studies demonstrated the major IGF-I mRNA splice variant, IGF-I Ea, increased over control levels during the myoblast differentiation phase. Moreover, a synthetic peptide corresponding the C-terminal 24 amino acids of human pro-IGF-I Ec reportedly stimulates mouse myoblast proliferation independently of the IGF-I receptor (Yang and Goldspink, 2002). These observations have led to the hypothesis that products of the IGF-I Eb mRNA spice variant [often termed mechano-growth factor (MGF)] mediates satellite cell proliferation whereas mature IGF-I, supposedly derived solely from expression of IGF-I Ea mRNA stimulates differentiation (See Barton, 2006; Matheny et al., 2010 for review).

The specific aim of the present study was to compare the time course of IGF-I gene expression, protein levels, and signaling cascades in the skeletal muscle of young and old mice following TK-induced I/R. We found clear age-related alterations in the relative quantities and temporal patterns of total IGF-I, IGF-I Ea, and IGF-I Eb gene expression in our model of injury. In addition, TK-injured aged skeletal muscle exhibits deficits in IGF-I peptide levels and anabolic signaling downstream of the IGF-I receptor. These data further support our hypothesis that an age-associated decrease in IGF-I induction following injury is a potential cause of the impaired regeneration of aged skeletal muscle.

METHODS

Animals

Young (6 mo) and old (24–28 mo) male C57BL/6 mice were used for this study. Animals were housed individually with *ad libitum* access to food and water, and maintained on a 12-hour light/dark cycle. Age-separated mice were randomly assigned into 1, 3, 5, and 7-day recovery groups (n = 5–6). All experimental procedures were approved and conducted in accordance with the guidelines set by The University of Texas at Austin IACUC.

Tourniquet Application

Mice were anesthetized with 2% isoflurane gas prior to and for the duration of tourniquet application. A single, randomly selected hind limb was elevated, and a pneumatic tourniquet (D.E. Hokanson, Inc.) was wrapped snuggly against the proximal portion of the limb and inflated to 250 mm Hg by the Portable Tourniquet System (Delfi Medical Innovations Inc.) to ensure complete occlusion of blood flow to the limb for a duration of 2 hours (Walters et al., 2008a). Body temperature was maintained at $37\pm1^{\circ}$ C with the use of a heat lamp during this procedure. After 2 hours, the pneumatic tourniquet was removed, and the mouse was returned to its cage for recovery. For all measures, muscles from the uninjured contralateral limb served as internal controls, as performed in other studies (Hammers et al., 2008; Thaveau et al., 2009; Walters et al., 2008b).

Tissue Harvesting

The gastrocnemius (GAS), tibialis anterior (TA), and extensor digitorum longus (EDL) muscles (muscles distal to the TK) were quickly harvested from both the TK and contralateral leg, and frozen in liquid nitrogen-cooled isopentane and stored at -80° C until later analysis. Plantaris (PLAN) muscles were fixed in 10% formalin for histological evaluation. Mice were euthanized with an overdose of sodium pentobarbital (100mg/kg).

Histological Analysis

Formalin-fixed PLAN muscle cross-sections were embedded in paraffin wax, cut 5 μm thick, and stained with hematoxylin & eosin (H&E). All slides were evaluated both subjectively and quantitatively by a board-certified veterinary pathologist using an Olympus BX41 microscope at 4, 10 and 40 X magnification. Images were captured at 40 X magnification using an Olympus BX41 microscope and an Olympus DP71 digital camera.

RT-PCR

Real-time PCR experiments were performed as previously described (Hammers et al., 2008). RNA was extracted from EDL muscles using RNA-STAT (Tel-Test, Friendswood, TX). Samples underwent chloroform extraction and centrifugation, followed by precipitation in isopropanol at -20° C. Precipitated RNA was centrifuged, the supernatant removed, and the pellet dissolved in nuclease-free water. RNA was quantified on a spectrophotometer at a wavelength of 260 nm. Conversion of total RNA to single-strand cDNA was accomplished using the High-Capacity cDNA Archive Kit (P/N 4322171; Applied Biosystems; Foster City, CA). Briefly, 5 – 10 μg total RNA were reverse transcribed using random primers for the following incubation times: 25º C for 10-minutes, then 37º C for 2 hours. cDNA samples were stored at -80° C until use.

RT-PCR was performed on cDNA using both commercially available (mouse 18S, ABI P/N Hs99999901_s1 and IGF-I, ABI P/N Mm00439561_m1, exon boundary 3–4) and custom-designed (See Table 1) hydrolysis primers and probes. The PCR reaction was performed in an ABI 7500 thermal cycler with the fluorescence of 3 to 15 cycles was set up as

background. Data was collected at the annealing step of each cycle, and the threshold cycle (Ct) for each sample calculated by determining the point at which the fluorescence exceeded the threshold limit. Standard curves for each probe/primer pair were established by serial 10-fold dilutions of cDNA of known concentrations, and the Ct values from samples were plotted along the curves to obtain relative values. All samples were then normalized to 18S rRNA. Data points represent the average of two to three runs, each in duplicate, and each performed on separate cDNA synthesis reactions.

ELISA

Tissue levels of IGF-I were measured by a method similar to that described by D'Ercole et al. (D'Ercole et al., 1984), with minor modifications. Briefly, ~100 mg of frozen muscle tissue (TA + EDL muscles) were powdered under liquid nitrogen and suspended in 5 mL of acetic acid per gram of tissue. Tissue suspensions were incubated on ice for 30 minutes and insoluble material was removed by centrifugation (10 minutes @ 5,000 g, 4º C). Extracts were lyophilized and resuspended in 0.1 M Tris (pH 8.0) at 2 mL/g of tissue. Samples were cleared by centrifugation (10 minutes @ 10,000 g, 4º C). Protein concentrations of cleared lysates were determined by the method described by Bradford (Bradford, 1976). An equal amount of protein was used to determine the IGF-I content using an IGF-I ELISA kit (Immuno Diagnostic Systems; Fountain Hills, AZ). Input volumes of the samples were increased to 25 μl, and the volume of diluent was decreased to 0.25 mL. The remainder of the assay was performed according to the manufacturer's instructions.

SDS-PAGE

Samples from control and TK GAS muscles (n = 5–6) were homogenized at 4º C in a buffer containing 50 mM HEPES (pH 7.6), 150 mM NaCl, 1% Triton-X 100, 20 mM β-glycerol phosphate, 10 mM NaF, 1 mM Na_3VO_4, 10 ng/mL each of leupeptin and aprotinin, 1 mM PMSF, and 1:100 dilutions of phosphatase inhibitor cocktails 1 & 2 (Sigma-Aldrich). The resulting homogenate was centrifuged at 12,000g for 30 minutes, and the supernatant was kept for analysis. Protein concentrations of all samples were determined as described by Bradford (1976). Samples were boiled in 4X Laemmli's sample buffer at a ratio of 3:1, and equal amounts of total protein were loaded into each well of a 5% stacking/15% separating polyacrylamide gel. Gels were run at constant current until necessary protein separation was achieved.

To verify equal loading of protein content among lanes, Coomassie blue staining of randomly selected gels was performed following SDS-PAGE separation. Gels were washed in dH$_2$O for 30 minutes, incubated in Bio-Safe Coomassie blue solution (Bio-Rad) for 1 hour, and washed again in dH$_2$O overnight. Gel images were taken using the Chemidoc XRS system (Bio-Rad). Volumetric analysis of all bands of each lane was performed using Quantity One software to verify that there were no substantial differences in total protein content despite differences in distribution of protein content between groups.

Western Blotting

Following SDS-PAGE separation, proteins were transferred to a PVDF membrane (Millipore) and blocked with 5% milk in 0.1% Tween 20 in TBS (TBST) for 1 hour. Ponceau-S staining was performed to ensure equal transfer prior to blocking. Membranes were incubated in 1:1000 dilutions of primary antibody in either 1% milk-TBST or 5% BSA-TBST overnight at 4° C, then in 1:2000 dilutions of goat anti-rabbit HRP conjugated secondary antibody (Pierce) in either 1% milk-TBST or 5% milk-TBST for 2 hours. Blots were visualized by ECL detection (Perkin-Elmer) using the Chemidoc XRS system (Bio-Rad). Band volumetric analysis was performed using Quantity One software. Following ECL detection of phospho-proteins, membranes were stripped and re-probed for total

protein. Anti-phospho-mTOR (Ser 2448; 2971), anti-phospho-FoxO3a (Ser 253; 9466), anti-Akt (9272), anti-mTOR (2972), and anti-FoxO3a (9467) primary antibodies were purchased from Cell Signaling Technology. Anti-phospo-Akt 1/2/3 (Ser 473; sc-7985-R) primary antibody was purchased from Santa Cruz Biotechnology. All experiments were repeated in triplicate to verify results.

Data Analysis

All values are expressed as mean ± SEM. Statistical analysis involved two-factor ANOVA (age and TK treatments; Student Newman-Keuls post-hoc tests) or Student's *t*-tests, where appropriate, using SPSS 16.0 software ($\alpha = 0.05$).

RESULTS

Muscle mass and histology

Figure 1 depicts the wet masses of all GAS muscles obtained in this study. In general, TK-injured muscles increased in mass 1 day post-TK, and this increase remained elevated through 3 days. Histological evidence confirmed this early post-TK increase coincides with edema and swelling of the myofibers. Following day 3, muscle masses of both age groups demonstrated progressive declines until day 7, when young and old muscles demonstrated significant decreases of 13 and 22% decreases in mass, respectively. At this time, the muscle mass of old mice was 27% lower than that of young. This decrease in old represents a 38% greater loss of mass, relative to day and age-matched controls, than the loss observed in young.

H&E stained PLAN muscle cross-sections from young and old 1, 3, 5, and 7-day recovery mice were evaluated by a board-certified veterinary pathologist to provide a histological comparison of the two age groups during the initial stages of recovery. Representative slides from each group are presented in Figure 2. Table 2 contains the mean histological pathology values for each group, as provided by the evaluator.

Control muscles from both young and old animals demonstrated no pathology, exhibiting angular fibers with peripheral nuclei. Following 1 day of recovery from I/R, old muscle demonstrated a higher degree of swelling (rounding of the myofibers), edema, neutrophil infiltration, and internalization of nuclei than young. Both age groups demonstrated a comparable degree of multifocal degeneration and necrosis. Similarly at day 3, old muscles demonstrated more myofiber swelling, edema, and infiltration of macrophages. Young muscles exhibited similar neutrophil infiltration as that observed in old, but revealed higher degrees of multifocal degeneration, necrosis, and internalized nuclei; neutrophil infiltration was similar to that of old. Old muscles in the 5-day recovery group exhibited similar degrees of degeneration/necrosis as those of young, yet had more severe instances of edema, infiltration of neutrophils and macrophages, and internalization of nuclei. Old muscles demonstrated a higher incidence of centrally located nuclei (i.e. regeneration) at this time, suggesting more damage had incurred. At 7 days, young and old muscles had similar degrees of edema, degeneration, and infiltration of neutrophils and macrophages; old muscles demonstrated higher amounts of swelling and regeneration than young at this time.

IGF-I gene expression

The local induction of IGF-I mRNA in skeletal muscle following an injury stimulus is well documented (Edwall et al., 1989; Hammers et al., 2008; Hill and Goldspink, 2003; Hill et al., 2003); however, its temporal regulation and the regulation of IGF-I splice variants is less clear. To address this, total IGF-I, IGF-I Ea, and IGF- I Eb mRNA in control and TK EDL muscles were measured by RT-PCR and were quantified relative to young 1 day control

values (Figure 3). Analysis of total IGF-I gene expression (Figure 3A) reveals both an age-related quantitative and temporal shift in the first 7 days following TK-induced I/R injury. TK-induced injury resulted in significant increases in IGF-I gene expression at days 1, 3, and 7 post-TK in both young, and at days 3, 5, and 7 in old compared to their respective controls. In young, IGF-I mRNA displayed a robust peak 3 days post-TK, while the old showed a delayed and quantitatively diminished peak at day 5. Old mice demonstrated significantly less TK-induced IGF-I gene expression than young at days 1 and 3, and was higher in expression at its peak on day 5. The expression of IGF-I Ea and Eb (Figure 3B & C, respectively) followed the same general pattern as total IGF-I gene expression. These data demonstrate temporal and quantitative impairment of IGF-I expression occurs with age following TK-induced injury.

Expression of myostatin (Figure 3D), a negative regulator of muscle mass (See Joulia-Ekaza and Cabello, 2007 for review) was also investigated. TK-induced injury resulted in substantial decreases in myostatin mRNA by for all time points in both young and old compared to their respective controls ($p \leq 0.05$), with that of old being lower in expression than young at days 1, 3, and 5 post-TK. This observed decrease in myostatin mRNA following I/R injury demonstrates that there was not a global up-regulation in RNA polymerase II-dependent gene transcription in response to I/R.

IGF-I peptide levels

Having observed that IGF-I mRNA decreased with age, we next sought to determine whether intramuscular immunoreactive IGF-I levels also decreased. A significant increase in IGF-I peptide following 7 days of recovery occurs in young, with no difference in old (Figure 4). These data indicate IGF-I peptide levels, in addition to mRNA, are reduced with age following TK-induced I/R.

Akt, mTOR, and FoxO3 signaling

To investigate the time-course of anabolic activity in young and old skeletal muscle following I/R, the phosphorylation of key proteins of the phosphoinositide 3-kinase (PI3K)/Akt pathway were analyzed (Figure 5). Early in recovery, levels of p-Akt and total Akt diminished to almost undetectable levels in both young and old, with no difference between the ages (Figure 5A). At day 5, p-Akt content rose in the young mice as total Akt increased ~3-fold over control values; however, the resulting p-Akt/Akt ratio was diminished. Old muscles still demonstrated no return of p-Akt signal. Values for p-Akt, total Akt, and p-Akt/Akt were significantly lower in the TK legs of old mice compared to their young counterparts at this time ($p \leq 0.05$). By day 7, there was an even more robust increase in total Akt in both age groups , however, p-Akt levels were higher in the young than old ($p \leq 0.05$). These data indicate an age-related delay in Akt synthesis and activation following I/R injury.

Mammalian target of rapamycin (mTOR) is a crucial mediator of anabolic activity in skeletal muscle (See Bodine, 2006 for review). There were no age-related differences in p-mTOR or mTOR among age groups until day 7 (Figure 5B). At this time, there were large increases in p-mTOR, mTOR, and p-mTOR/mTOR values in the young mice relative to day-matched control levels. The p-mTOR and mTOR values were significantly higher than those of old mice ($p \leq 0.05$), suggesting synthesis and subsequent phosphorylation of mTOR is impaired/delayed in aged muscle recovering from I/R.

The FoxO class transcription factors (FoxOs) are targets of active Akt kinase activity. In their active, unphosphorylated state, these proteins reside in the nucleus and promote gene expression of atrophy-stimulating genes, such as the E3 ubiquitin ligase, atrogin-1 (Sandri et

al., 2004). Phosphorylation of FoxOs by Akt induces translocation from the nucleus and degradation in the cytosol (See Huang and Tindall, 2007 for review). Content of p-FoxO3 followed the same pattern as p-mTOR (Figure 5C). After 7 days of recovery, p-FoxO3 content in young was substantially higher than old, while total FoxO3 levels were well below those of old ($p \leq 0.05$). The depressed p-FoxO3/FoxO3 ratio in old ($p \leq 0.05$) indicates more active, atrophy-inducing FoxO3 in the muscle of old mice. The physiological relevance of these signaling deficits are strengthened by the exacerbated loss of mass in the muscles of old following TK application (Figure 1, Day 7).

DISCUSSION

The substantial loss of muscle mass and function that result from TK use are a concern among the high proportion of elderly individuals who undergo orthopedic surgery, as muscle mass and strength are negatively associated with disability and mortality rates (See Rantanen, 2003 for review). The data presented in this study demonstrate clear age-related alterations in local IGF-I gene expression, IGF-I peptide levels, and anabolic signaling in skeletal muscle following I/R in mice. In this study we present several novel findings including a correlation between IGF-I mRNA levels and protein levels in aged muscle and a reduction in intracellular signals generated by the IGF-I receptor. In addition, we find an elevation in potentially active FoxO in the muscle of aged animals. These novel findings extend our previous observations and provide important information regarding the potential mechanisms that underlie the reduced capacity for aged muscle to recover from injury.

Due to its pleiotrophic effects, IGF-I is an important molecule in the study of skeletal muscle response to injury. IGF-I stimulates both the proliferation and differentiation of myoblasts via activation of the MAP kinase and PI3K/Akt pathways, respectively (Coolican et al., 1997). In differentiated muscle, IGF-I is hypertrophic and anti-atrophic, with both actions largely attributed to PI3K/Akt activation (Adams and McCue, 1998; Latres et al., 2005; Lee et al., 2004; Rommel et al., 2001; Sacheck et al., 2004; Stitt et al., 2004). IGF-I overexpression also increases the recruitment of circulating bone marrow-derived stem cells (Musaro et al., 2004; Sacco et al., 2005) and hastens the resolution of inflammation (Pelosi et al., 2007) following muscle injury. Additional benefits of IGF-I may include protection of cells from oxidative stress (Garcia-Fernandez et al., 2005; Jallali et al., 2007), mitochondrial dysfunction (Puche et al., 2008), and apoptosis (See Kooijman, 2006 for review), as seen in non-muscle tissues.

Due to the positive effects of IGF-I, we hypothesize that the age-related impairment of IGF-I expression is a contributing factor to the general decrement of aged muscle following injury. This is supported by evidence that the forced overexpression of IGF-I in the skeletal muscles of aged mice prevents the sarcopenic phenotype (Barton-Davis et al., 1998; Musaro et al., 2001) and protects injured muscles from the exacerbated decrement caused by aging (Musaro et al., 2001). In addition, the administration of IGF-I has the ability to restore the proliferative potential of satellite cells in atrophied aged muscles (Chakravarthy et al., 2000). Despite these effects of IGF-I on sarcopenia, it was only recently shown that the post-injury expression of IGF-I decreases with age (Hammers et al., 2008). The present study verifies this age-related reduction in the injury-induced IGF-I expression exists in the mouse model of TK-induced I/R with the distinctive finding that a delay in peak expression also occurs, as young peak in expression at 3 days post-TK and old at 5 days post-TK. We also verify that IGF-I peptide levels are reduced with age. The merits of these findings are further strengthened by recent evidence that functional IGF-I receptors are required for the efficient regeneration of injured skeletal muscle, thereby highlighting the importance of IGF-I to muscle regeneration (Heron-Milhavet et al., 2010). This current line of evidence suggests

that non-genetic, IGF-I-based intervention may be an effective method of therapeutic intervention.

An interesting finding of this study is the lack of differential expression of the IGF-I Ea and Eb isoforms. The works of Hill et al. suggest that local expression of the individual IGF-I Ea and Eb mRNA splice variants is temporally specific following some models of muscle injury. For instance, increases of the IGF-I Eb splice variant beyond control levels coincided temporally with the proliferation of satellite cells, and increases of the IGF-I Ea splice variant beyond control levels coincided temporally with myoblast differentiation (Hill and Goldspink, 2003; Hill et al., 2003). Owino et al. (2001) reported that old rats exhibited an attenuated up-regulation of IGF-I Eb mRNA at 1–5 days following overload compared to young rats, and that the lower induction of IGF-I Eb mRNA in the older rats correlated with attenuation in appearance of myogenesis markers. These findings led the authors to speculate that protein product(s) derived from IGF-I Eb mRNA may be involved in satellite cell activation, and that product(s) derived from IGF-I Ea mRNA may be involved in differentiation. A synthetic peptide corresponding to the 24 C-terminal amino acids of the Eb E peptide stimulated proliferation and inhibited differentiation of C2C12 cells (Yang and Goldspink, 2002). Because antibodies raised against this sequence have detected proteins larger than the intact Eb peptide or the 24-aa C-terminal fragment (Dluzniewska et al., 2005; Kravchenko et al., 2006; Philippou et al., 2008) and no published reports exist where this IGF-I Eb mRNA product has been identified in, or isolated from, injured tissues *in vivo* , the identity of the precise form or physiological role of MGF remains elusive.

Here, we observe an increased level of immunoreactive IGF-I in association with increased levels of both IGF-I Ea and IGF-I Eb mRNAs, and an attenuation of both IGF-I mRNA splice variants and of immunoreactive IGF-I in older mice following I/R. Our results thus do not indicate temporal specificity of Ea and Eb following I/R. The discrepancy between our findings and those of Hill et al. may be due to a difference in the nature of the injury models. The bupivacaine-induced muscle injury used by Hill et al. is specific to mature myofibers, and does not substantially affect non-muscle cells, such as the surrounding vasculature or nerve cells (Foster and Carlson, 1980). Non-muscle cells, however, are affected in the I/R model and express IGF-I following this perturbation (Jennische et al., 1987), thus their contributions may change the landscape of local IGF-I gene expression.

The skeletal muscle of aged mice also demonstrate significant deficits in phosphorylation of Akt, mTOR, and FoxO3, all indicators of positive anabolic activity, compared to their young counterparts after 7 days of recovery from TK-induced I/R. Activation of the PI3K/Akt pathway leads to an increase in protein synthesis through a mTOR-dependent process (Bodine et al., 2001; Rommel et al., 2001), and prevents atrophy through a mostly FoxO-dependent process (Sandri et al., 2004). Indirect activation of mTOR by Akt initiates the activation of pro-translational signaling by the activation p70 S6 Kinase (p70^{S6K}) and the deactivation of 4E-Binding Protein (4E-BP) through phosphorylation (Bodine et al., 2001; Burnett et al., 1998). The reduction of pAkt and pmTOR in old muscle suggests protein synthetic pathways are attenuated with age following I/R. A similar delayed response of Akt activation in old rats was recently found to coincide with impaired hypertrophy using the functional overload model (Hwee and Bodine, 2009). The present data indicates that the mechanism responsible for the age-related decrease in signaling is prior to the activation of Akt, perhaps due to changes in IGF-I ligand levels. We are, however, limited by the fact that different muscles were used for mRNA/peptide and signaling assays. We also cannot, at this time, discount the possibility of age-related alterations in the expression and/or activation of upstream mediators of Akt activation, such as IGF-IR, IRS-1, and/or PI3K, or proteins downstream of mTOR, including mTORC1, p70^{S6K}, 4E-BP, and/or ribosomal protein S 6.

Another important finding of the current study is the substantially reduced pFoxO3/FoxO3 levels in the TK muscles of old mice. In differentiated muscle, active FoxO proteins are localized in the nucleus and activate transcription of the muscle-specific E3 ubiquitin ligases Atrogin-1 and MuRF-1 (Sandri et al., 2004; Senf et al., 2008; Stitt et al., 2004) and many genes associated with autophagy (Mammucari et al., 2007; Sengupta et al., 2009; Zhao et al., 2007), causing substantial atrophy. In addition, FoxOs are responsible for the upregulation of the cell cycle inhibitor p27^{kip1}, thereby preventing satellite cell proliferation (Machida et al., 2003; Rathbone et al., 2008). FoxOs have also been shown to induce apoptosis *in vitro* (Matheny and Adamo, 2009; McLoughlin et al., 2009). IGF-I mediated phosphorylation of FoxOs by Akt causes their exclusion from the nucleus, thereby preventing their transcriptional activity (Sandri et al., 2004; Stitt et al., 2004). These data suggest FoxO activity is elevated in TK-injured aged muscle, leading to an age-related increase in atrophy stimulation and/or reduced proliferative potential of satellite cells.

In summary, the present data demonstrate that the local induction of IGF-I gene expression, IGF-I peptide levels, and signaling of the PI3K/Akt pathway in skeletal muscle are attenuated with age following 2 hour TK-induced I/R injury. This result is clinically significant due to the growing elderly population and the large proportion of orthopedic surgeries within this demographic. However, further investigation needs to address the mechanisms behind the age-related reduction in IGF-I response, i.e. whether it is due to extrinsic factors, intrinsic phenomena, or an interaction thereof. Despite this, the results of this study strengthen the use of IGF-I based therapy as a potential treatment to promote normal regeneration in the injured skeletal muscle of aged individuals.

Research Highlights

- Aging muscle incurs greater damage following tourniquet-induced I/R than young muscle

- IGF-I expression in both peptide and mRNA of splice variants of IGF-I Ea and Eb were reduced in aging

- Anabolic activity of aged muscle subsequent to injury was reduced compared to young

- Phosphorylation of select intermediates of the PI3 Kinase pathway were reduced in aged muscle

Impairment of IGF-I signaling in aging potentially has a role in impaired recovery in aged muscle

Acknowledgments

References

Adamo ML, Farrar RP. Resistance training, and IGF involvement in the maintenance of muscle mass during the aging process. Ageing Res Rev. 2006; 5:310–31. [PubMed: 16949353]

Conboy IM, Rando TA. Aging, stem cells and tissue regeneration: lessons from muscle. Cell Cycle. 2005; 4:407–10. [PubMed: 15725724]

Brooks SV, Faulkner JA. The magnitude of the initial injury induced by stretches of maximally activated muscle fibres of mice and rats increases in old age. J Physiol. 1996; 497 (Pt 2):573–80. [PubMed: 8961197]

Zerba E, Komorowski TE, Faulkner JA. Free radical injury to skeletal muscles of young, adult, and old mice. Am J Physiol. 1990; 258:C429–35. [PubMed: 2316631]

Brooks SV, Faulkner JA. Contraction-induced injury: recovery of skeletal muscles in young and old mice. Am J Physiol. 1990; 258:C436–42. [PubMed: 2316632]

Hammers DW, Merritt EK, Matheny W, Adamo ML, Walters TJ, Estep JS, Farrar RP. Functional deficits and insulin-like growth factor-I gene expression following tourniquet-induced injury of skeletal muscle in young and old rats. J Appl Physiol. 2008; 105:1274–81. [PubMed: 18669936]

Sadeh M. Effects of aging on skeletal muscle regeneration. J Neurol Sci. 1988; 87:67–74. [PubMed: 3193124]

Carlson BM, Faulkner JA. Muscle transplantation between young and old rats: age of host determines recovery. Am J Physiol. 1989; 256:C1262–6. [PubMed: 2735398]

Conboy IM, Conboy MJ, Wagers AJ, Girma ER, Weissman IL, Rando TA. Rejuvenation of aged progenitor cells by exposure to a young systemic environment. Nature. 2005; 433:760–4. [PubMed: 15716955]

McEwen JA, Inkpen K. Surgical Tourniquet Technology Adapted for Military and Prehospital Use. RTO-MP-HFM. 2004; 109:1–12.

Blaisdell FW. The pathophysiology of skeletal muscle ischemia and the reperfusion syndrome: a review. Cardiovasc Surg. 2002; 10:620–30. [PubMed: 12453699]

Edwall D, Schalling M, Jennische E, Norstedt G. Induction of insulin-like growth factor I messenger ribonucleic acid during regeneration of rat skeletal muscle. Endocrinology. 1989; 124:820–5. [PubMed: 2912704]

Hayashi S, Aso H, Watanabe K, Nara H, Rose MT, Ohwada S, Yamaguchi T. Sequence of IGF-I, IGF-II, and HGF expression in regenerating skeletal muscle. Histochem Cell Biol. 2004; 122:427–34. [PubMed: 15480739]

Hill M, Goldspink G. Expression and splicing of the insulin-like growth factor gene in rodent muscle is associated with muscle satellite (stem) cell activation following local tissue damage. J Physiol. 2003; 549:409–18. [PubMed: 12692175]

Hill M, Wernig A, Goldspink G. Muscle satellite (stem) cell activation during local tissue injury and repair. J Anat. 2003; 203:89–99. [PubMed: 12892408]

Jennische E, Hansson HA. Regenerating skeletal muscle cells express insulin-like growth factor I. Acta Physiol Scand. 1987; 130:327–32. [PubMed: 3300170]

Jennische E, Skottner A, Hansson HA. Satellite cells express the trophic factor IGF-I in regenerating skeletal muscle. Acta Physiol Scand. 1987; 129:9–15. [PubMed: 3551503]

Adams GR. Autocrine and/or paracrine insulin-like growth factor-I activity in skeletal muscle. Clin Orthop Relat Res. 2002:S188–96. [PubMed: 12394468]

Charge SB, Rudnicki MA. Cellular and molecular regulation of muscle regeneration. Physiol Rev. 2004; 84:209–38. [PubMed: 14715915]

Yang SY, Goldspink G. Different roles of the IGF-I Ec peptide (MGF) and mature IGF-I in myoblast proliferation and differentiation. FEBS Lett. 2002; 522:156–60. [PubMed: 12095637]

Barton ER. The ABCs of IGF-I isoforms: impact on muscle hypertrophy and implications for repair. Appl Physiol Nutr Metab. 2006; 31:791–7. [PubMed: 17213901]

Matheny RW Jr, Nindl BC, Adamo ML. Minireview: Mechano-growth factor: a putative product of IGF-I gene expression involved in tissue repair and regeneration. Endocrinology. 2010; 151:865–75. [PubMed: 20130113]

Walters TJ, Kragh JF, Kauvar DS, Baer DG. The combined influence of hemorrhage and tourniquet application on the recovery of muscle function in rats. J Orthop Trauma. 2008a; 22:47–51. [PubMed: 18176165]

Thaveau F, Zoll J, Bouitbir J, Ribera F, Di Marco P, Chakfe N, Kretz JG, Piquard F, Geny B. Contralateral leg as a control during skeletal muscle ischemia-reperfusion. J Surg Res. 2009; 155:65–9. [PubMed: 19159910]

Walters TJ, Kragh JF, Baer DG. Influence of fiber-type composition on recovery from tourniquet-induced skeletal muscle ischemia-reperfusion injury. Appl Physiol Nutr Metab. 2008b; 33:272–81. [PubMed: 18347682]

D'Ercole AJ, Stiles AD, Underwood LE. Tissue concentrations of somatomedin C: further evidence for multiple sites of synthesis and paracrine or autocrine mechanisms of action. Proc Natl Acad Sci U S A. 1984; 81:935–9. [PubMed: 6583688]

Bradford MM. A rapid and sensitive method for the quantitation of microgram quantities of protein utilizing the principle of protein-dye binding. Anal Biochem. 1976; 72:248–54. [PubMed: 942051]

Joulia-Ekaza D, Cabello G. The myostatin gene: physiology and pharmacological relevance. Curr Opin Pharmacol. 2007; 7:310–5. [PubMed: 17374508]

Bodine SC. mTOR signaling and the molecular adaptation to resistance exercise. Med Sci Sports Exerc. 2006; 38:1950–7. [PubMed: 17095929]

Sandri M, Sandri C, Gilbert A, Skurk C, Calabria E, Picard A, Walsh K, Schiaffino S, Lecker SH, Goldberg AL. Foxo transcription factors induce the atrophy-related ubiquitin ligase atrogin-1 and cause skeletal muscle atrophy. Cell. 2004; 117:399–412. [PubMed: 15109499]

Huang H, Tindall DJ. Dynamic FoxO transcription factors. J Cell Sci. 2007; 120:2479–87. [PubMed: 17646672]

Rantanen T. Muscle strength, disability and mortality. Scand J Med Sci Sports. 2003; 13:3–8. [PubMed: 12535311]

Coolican SA, Samuel DS, Ewton DZ, McWade FJ, Florini JR. The mitogenic and myogenic actions of insulin-like growth factors utilize distinct signaling pathways. J Biol Chem. 1997; 272:6653–62. [PubMed: 9045696]

Adams GR, McCue SA. Localized infusion of IGF-I results in skeletal muscle hypertrophy in rats. J Appl Physiol. 1998; 84:1716–22. [PubMed: 9572822]

Latres E, Amini AR, Amini AA, Griffiths J, Martin FJ, Wei Y, Lin HC, Yancopoulos GD, Glass DJ. Insulin-like growth factor-1 (IGF-1) inversely regulates atrophy-induced genes via the phosphatidylinositol 3-kinase/Akt/mammalian target of rapamycin (PI3K/Akt/mTOR) pathway. J Biol Chem. 2005; 280:2737–44. [PubMed: 15550386]

Lee S, Barton ER, Sweeney HL, Farrar RP. Viral expression of insulin-like growth factor-I enhances muscle hypertrophy in resistance-trained rats. J Appl Physiol. 2004; 96:1097–104. [PubMed: 14766764]

Rommel C, Bodine SC, Clarke BA, Rossman R, Nunez L, Stitt TN, Yancopoulos GD, Glass DJ. Mediation of IGF-1-induced skeletal myotube hypertrophy by PI(3)K/Akt/mTOR and PI(3)K/Akt/GSK3 pathways. Nat Cell Biol. 2001; 3:1009–13. [PubMed: 11715022]

Sacheck JM, Ohtsuka A, McLary SC, Goldberg AL. IGF-I stimulates muscle growth by suppressing protein breakdown and expression of atrophy-related ubiquitin ligases, atrogin-1 and MuRF1. Am J Physiol Endocrinol Metab. 2004; 287:E591–601. [PubMed: 15100091]

Stitt TN, Drujan D, Clarke BA, Panaro F, Timofeyva Y, Kline WO, Gonzalez M, Yancopoulos GD, Glass DJ. The IGF-1/PI3K/Akt pathway prevents expression of muscle atrophy-induced ubiquitin ligases by inhibiting FOXO transcription factors. Mol Cell. 2004; 14:395–403. [PubMed: 15125842]

Musaro A, Giacinti C, Borsellino G, Dobrowolny G, Pelosi L, Cairns L, Ottolenghi S, Cossu G, Bernardi G, Battistini L, Molinaro M, Rosenthal N. Stem cell-mediated muscle regeneration is enhanced by local isoform of insulin-like growth factor 1. Proc Natl Acad Sci U S A. 2004; 101:1206–10. [PubMed: 14745025]

Sacco A, Doyonnas R, LaBarge MA, Hammer MM, Kraft P, Blau HM. IGF-I increases bone marrow contribution to adult skeletal muscle and enhances the fusion of myelomonocytic precursors. J Cell Biol. 2005; 171:483–92. [PubMed: 16275752]

Pelosi L, Giacinti C, Nardis C, Borsellino G, Rizzuto E, Nicoletti C, Wannenes F, Battistini L, Rosenthal N, Molinaro M, Musaro A. Local expression of IGF-1 accelerates muscle regeneration by rapidly modulating inflammatory cytokines and chemokines. Faseb J. 2007; 21:1393–402. [PubMed: 17264161]

Garcia-Fernandez M, Castilla-Cortazar I, Diaz-Sanchez M, Navarro I, Puche JE, Castilla A, Casares AD, Clavijo E, Gonzalez-Baron S. Antioxidant effects of insulin-like growth factor-I (IGF-I) in rats with advanced liver cirrhosis. BMC Gastroenterol. 2005; 5:7. [PubMed: 15745444]

Jallali N, Ridha H, Thrasivoulou C, Butler P, Cowen T. Modulation of intracellular reactive oxygen species level in chondrocytes by IGF-1, FGF, and TGF-beta1. Connect Tissue Res. 2007; 48:149–58. [PubMed: 17522998]

Puche JE, Garcia-Fernandez M, Muntane J, Rioja J, Gonzalez-Baron S, Castilla Cortazar I. Low doses of insulin-like growth factor-I induce mitochondrial protection in aging rats. Endocrinology. 2008; 149:2620–7. [PubMed: 18276748]

Kooijman R. Regulation of apoptosis by insulin-like growth factor (IGF)-I. Cytokine Growth Factor Rev. 2006; 17:305–23. [PubMed: 16621671]

Barton-Davis ER, Shoturma DI, Musaro A, Rosenthal N, Sweeney HL. Viral mediated expression of insulin-like growth factor I blocks the aging-related loss of skeletal muscle function. Proc Natl Acad Sci U S A. 1998; 95:15603–7. [PubMed: 9861016]

Musaro A, McCullagh K, Paul A, Houghton L, Dobrowolny G, Molinaro M, Barton ER, Sweeney HL, Rosenthal N. Localized Igf-1 transgene expression sustains hypertrophy and regeneration in senescent skeletal muscle. Nat Genet. 2001; 27:195–200. [PubMed: 11175789]

Chakravarthy MV, Davis BS, Booth FW. IGF-I restores satellite cell proliferative potential in immobilized old skeletal muscle. J Appl Physiol. 2000; 89:1365–79. [PubMed: 11007571]

Heron-Milhavet L, Mamaeva D, LeRoith D, Lamb NJ, Fernandez A. Impaired muscle regeneration and myoblast differentiation in mice with a muscle-specific KO of IGF-IR. J Cell Physiol. 2010; 225:1–6. [PubMed: 20458740]

Owino V, Yang SY, Goldspink G. Age-related loss of skeletal muscle function and the inability to express the autocrine form of insulin-like growth factor-1 (MGF) in response to mechanical overload. FEBS Lett. 2001; 505:259–63. [PubMed: 11566187]

Dluzniewska J, Sarnowska A, Beresewicz M, Johnson I, Srai SK, Ramesh B, Goldspink G, Gorecki DC, Zablocka B. A strong neuroprotective effect of the autonomous C-terminal peptide of IGF-1 Ec (MGF) in brain ischemia. Faseb J. 2005; 19:1896–8. [PubMed: 16144956]

Kravchenko IV, Furalyov VA, Khotchenkov VP, Popov VO. Monoclonal antibodies to mechano-growth factor. Hybridoma (Larchmt). 2006; 25:300–5. [PubMed: 17044786]

Philippou A, Stavropoulou A, Sourla A, Pissimissis N, Halapas A, Maridaki M, Koutsilieris M. Characterization of a rabbit antihuman mechano growth factor (MGF) polyclonal antibody against the last 24 amino acids of the E domain. In Vivo. 2008; 22:27–35. [PubMed: 18396778]

Foster AH, Carlson BM. Myotoxicity of local anesthetics and regeneration of the damaged muscle fibers. Anesth Analg. 1980; 59:727–36. [PubMed: 7191645]

Bodine SC, Stitt TN, Gonzalez M, Kline WO, Stover GL, Bauerlein R, Zlotchenko E, Scrimgeour A, Lawrence JC, Glass DJ, Yancopoulos GD. Akt/mTOR pathway is a crucial regulator of skeletal muscle hypertrophy and can prevent muscle atrophy in vivo. Nat Cell Biol. 2001; 3:1014–9. [PubMed: 11715023]

Burnett PE, Barrow RK, Cohen NA, Snyder SH, Sabatini DM. RAFT1 phosphorylation of the translational regulators p70 S6 kinase and 4E-BP1. Proc Natl Acad Sci U S A. 1998; 95:1432–7. [PubMed: 9465032]

Hwee DT, Bodine SC. Age-related deficit in load-induced skeletal muscle growth. J Gerontol A Biol Sci Med Sci. 2009; 64:618–28. [PubMed: 19351696]

Senf SM, Dodd SL, McClung JM, Judge AR. Hsp70 overexpression inhibits NF-kappaB and Foxo3a transcriptional activities and prevents skeletal muscle atrophy. Faseb J. 2008; 22:3836–45. [PubMed: 18644837]

Mammucari C, Milan G, Romanello V, Masiero E, Rudolf R, Del Piccolo P, Burden SJ, Di Lisi R, Sandri C, Zhao J, Goldberg AL, Schiaffino S, Sandri M. FoxO3 controls autophagy in skeletal muscle in vivo. Cell Metab. 2007; 6:458–71. [PubMed: 18054315]

Sengupta A, Molkentin JD, Yutzey KE. FoxO transcription factors promote autophagy in cardiomyocytes. J Biol Chem. 2009; 284:28319–31. [PubMed: 19696026]

Zhao J, Brault JJ, Schild A, Cao P, Sandri M, Schiaffino S, Lecker SH, Goldberg AL. FoxO3 coordinately activates protein degradation by the autophagic/lysosomal and proteasomal pathways in atrophying muscle cells. Cell Metab. 2007; 6:472–83. [PubMed: 18054316]

Machida S, Spangenburg EE, Booth FW. Forkhead transcription factor FoxO1 transduces insulin-like growth factor's signal to p27Kip1 in primary skeletal muscle satellite cells. J Cell Physiol. 2003; 196:523–31. [PubMed: 12891709]

Rathbone CR, Booth FW, Lees SJ. FoxO3a preferentially induces p27Kip1 expression while impairing muscle precursor cell-cycle progression. Muscle Nerve. 2008; 37:84–9. [PubMed: 17894357]

Matheny RW Jr, Adamo ML. Role of Akt isoforms in IGF-I-mediated signaling and survival in myoblasts. Biochem Biophys Res Commun. 2009; 389:117–21. [PubMed: 19703413]

McLoughlin TJ, Smith SM, DeLong AD, Wang H, Unterman TG, Esser KA. FoxO1 induces apoptosis in skeletal myotubes in a DNA-binding-dependent manner. Am J Physiol Cell Physiol. 2009; 297:C548–55. [PubMed: 19553561]
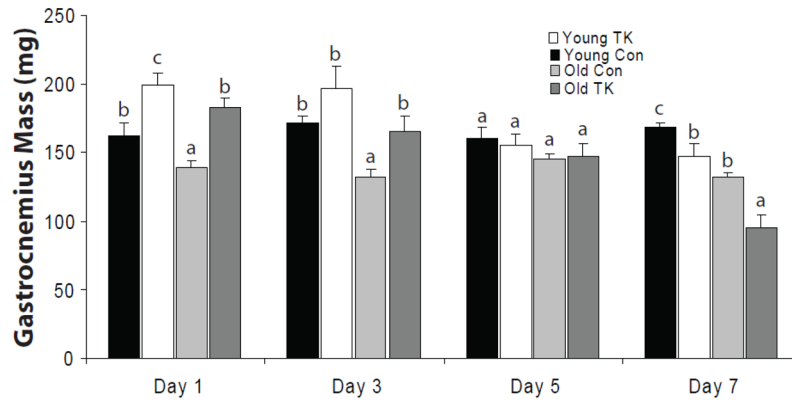
Figure 1.
Wet masses of gastrocnemius muscles were measured from 6 mo (young) and 24–27 mo (old) C57BL/6 mice following 1, 3, 5, and 7 days of recovery from 2 hour TK-induced I/R. Values are represented as mean ± SEM. Statistical analysis was performed using two-factor ANOVA followed by SNK post-hoc (α = 0.05).
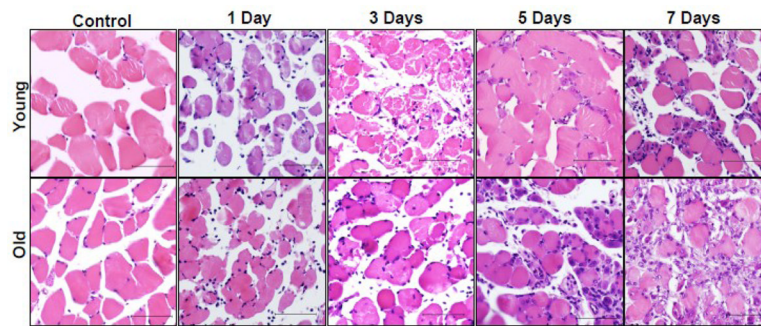
Figure 2.
Plantaris muscles from 6 mo (young) and 24–27 mo (old) C57BL/6 mice were paraffin-embedded and stained with hematoxylin & eosin (H&E) following 1, 3, 5, and 7 days of recovery from 2 hour TK-induced I/R. Inset bar represents 100 μm.
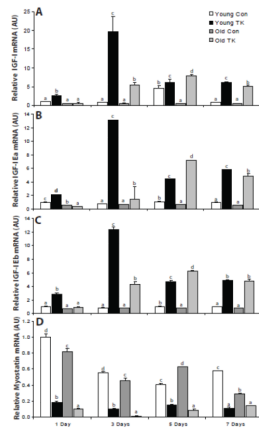
Figure 3.
Real time-PCR was performed to measure relative expression of IGF-I (**A**), IGF-I Ea (**B**), IGF-I Eb (**C**), and myostatin (**D**) mRNA in the extensor digitorum longus muscle of 6 mo (young) and 24–27 mo (old) C57BL/6 mice following 1, 3, 5, and 7 days of recovery from 2 hour TK-induced I/R. mRNA values are normalized to 18S rRNA expression and are represented as mean ± SEM relative to Day 1 young control levels. Statistical analysis was performed using two-factor ANOVA followed by SNK post-hoc (α = 0.05).
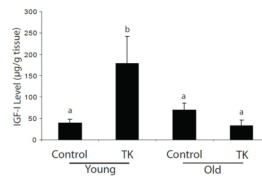
Figure 4.
Whole tissue IGF-I peptide levels were measured by ELISA in the tibialis anterior and extensor digitorum longus muscles of 6 mo (young) and 24–27 mo (old) C57BL/6 mice following 7 days recovery from TK-induced I/R. Values are represented as mean ± SEM. Statistical analysis was performed using two-factor ANOVA followed by SNK post-hoc (α = 0.05).
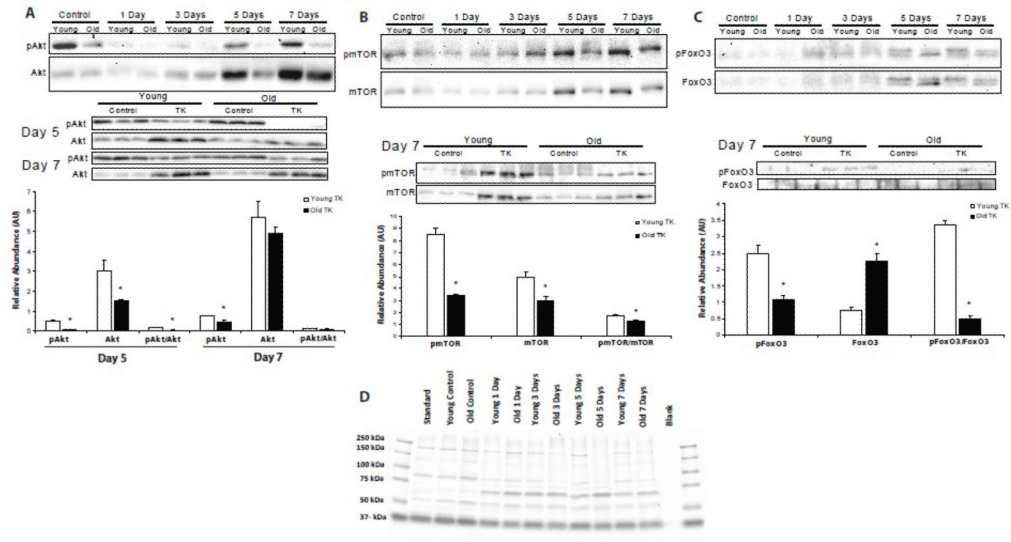
Figure 5.
Relative phosphorylation abundances, total protein contents, and phosphorylation/total protein ratios of Akt (**A**), mTOR (**B**), and FoxO3 (**C**) were measured by Western blotting samples from the gastrocnemius muscle of 6 mo (young) and 24–27 mo (old) C57BL/6 mice following TK-induced I/R. Representative Coomassie-blue stained gel (**D**) demonstrates consistent loading in all SDS-PAGE experiments. Values are represented as mean ± SEM. Statistical analysis was performed using Student's *t*-tests; * p ≤ 0.05.

Table 1

RT-PCR primers

	Forward	Reverse	Probe (Exon Boundary)
IGF-I Ea	CCACACTGACATGCCCAAGA	CCTGCACTTCCTCTACTTGTGTTC	TCAGAAGGAAGTACATTTGA (4–6)
IGF-I Eb	CCACACTGACATGCCCAAGAC	GCTTCGTTTTCTTGTTTGTCGAT	AGAAGTCCCCGTCCC (4–5)
Myostatin	TACCACGGAAACAATCATTACCAT	TGCCATCCGCTTGCATT	CTACAGAGTCTGACTTTCT (2–3)

Table 2

Pathological evalutation of H&E stained plantaris muscles

	Control		1 Day		3 Days		5 Days		7 Days	
	Young	Old	Young	Old	Young	Old	Young	Old	Young	Old
Muscle Pathology										
Degeneration										
area of slide	0.0	0.1±0.0	3.3±0.3	4.0±0.0	4.0±0.0	2.7±0.8	2.7±0.6	2.5±0.7	1.4±0.5	1.2±0.5
severity			*min-mod*	*min-mod*	*min-mod*	*mld-sev*	*min-mod*	*min-mod*	*min*	*min-mld*
Necrosis	0.0	0.0	1.0±0.3	1.3±0.6	1.7±0.7	1.5±0.7	0.8±0.5	0.7±0.4	0.1±0.1	0.0
Edema	0.0	0.0	1.5±0.4	2.3±0.3	1.7±0.4	1.2±0.4	0.7±0.5	0.5±0.3	0.1±0.1	0.2±0.2
Fibrosis	0.0	0.0	0.0	0.0	0.0	0.0	0.6±0.4	1.5±0.5	1.7±0.4	2.0±0.3
Hemorrhage	0.0	0.0	0.3±0.2	1.7±0.5	2.5±0.3	0.7±0.3	1.3±0.5	2.3±0.2	0.0	0.2±0.2
Regeneration	0.0	0.0	0.0	0.0	0.0	0.0	1.2±0.6	3.2±0.7	2.9±0.6	4.0±0.0
Inflammation										
Neutrophils	0.0	0.0	2.0±0.3	2.7±0.2	2.2±0.5	1.7±0.6	1.0±0.4	1.8±0.3	0.3±0.2	0.2±0.2
Macrophages	0.0	0.0	0.3±0.2	0.5±0.2	1.0±0.5	0.7±0.4	1.7±0.6	2.3±0.3	1.0±0.3	1.6±0.4
Lymphocytes/plasma cells	0.0	0.0	0.3±0.2	0.2±0.2	0.5±0.3	0.0	0.8±0.4	1.7±0.2	1.7±0.2	1.6±0.4

For measures of degeneration and necrosis: 0 = normal muscle, 1 = 0–5%, 2 = 5–20%, 3 = 20–40%, and 4 = >40% of slide area; severity of degeneration is denoted as min (minimal), mld (mild), mod (moderate), or sev (severe). For edema, hemorrhage, fibrosis, neutrophils, macrophages, and lymphocytes/plasma cells: 0 = normal, 1= minimal, 2 = mild, 3 = moderate, and 4 = severe. Values indicated are means ± SE.